Review of the Current Status of Four-Dimensional Ionospheric Imaging

G.S. Bust
Applied Research Laboratories
The University of Texas at Austin
USA

gbust@arlut.utexas.edu

C.N. Mitchell
Dept. of Electronic and Electrical Engineering
University of Bath
UK

c.n.Mitchell@bath.ac.uk

ABSTRACT

Recent developments in tomographic imaging allow the use of GPS satellite data to image the Earth's ionosphere. Ground-based GPS receivers monitor the Earth's ionosphere continuously and a comprehensive database of ionospheric measurements suitable for tomographic processing now exists. The tomographic inversion of these GPS data in a three-dimensional time-dependent inversion algorithm can reveal the spatial and temporal distribution of ionospheric electron density. This new technique is unique for studying ionospheric physics because it gives a time-continuous near-global view of the ionosphere. The tomographic algorithms have been under continuous development for several years and are now yielding new geophysical results.

1.0 INTRODUCTION

In 1986 a new technique for ionospheric study was proposed, namely radio tomography. Section 2 includes a review of ionospheric tomography, while Section 3 describes current developments in ionospheric imaging and practical applications of the work. Initial research established the validity of the technique by comparisons between co-located tomographic images and incoherent scatter radar observations. Tomographic images have now revealed a number of physical processes in the ionosphere, some of which are signatures of events originating in the magnetosphere. Recent work has shown the potential to extend the algorithms to make three- and four-dimensional images (movies) using multiple satellites and receivers. Radio tomography and inversion imaging offer powerful new methods for the routine monitoring of the near-Earth space-plasma. In addition to scientific investigations, the research has important applications in improving radio communication and navigation systems. Section 4 outlines current limitations and future directions for this particular research topic. These future directions fall into two areas. Firstly, a number of new satellites are being launched that will provide increased global coverage and opportunities for improved, higher resolution imaging. Secondly, the prospect of incorporating mathematical inversion theory into physical models of the solar-terrestrial regions to better understand the underlying physics that is producing the images.

2.0 HISTORY OF IONOSPHERIC TOMOGRAPHY AND IMAGING

The tomographic technique Radon (1917),, so successful in the medical field, has been applied relatively recently to producing images of the electron concentration in the ionosphere. This has been done using a polar-orbiting satellite as the transmitter platform, together with arrays of receivers on the ground. Dual frequency trans-ionospheric signals are analysed and inverted using an algorithm to produce two-dimensional images of electron concentration. This application of tomography to the ionosphere falls into the category of

Bust, G.S.; Mitchell, C.N. (2006) Review of the Current Status of Four-Dimensional Ionospheric Imaging. In *Characterising the Ionosphere* (pp. 31-1 – 31-18). Meeting Proceedings RTO-MP-IST-056, Paper 31. Neuilly-sur-Seine, France: RTO. Available from: http://www.rto.nato.int/abstracts.asp.

Report Documentation Page

Form Approved
OMB No. 0704-0188

1. REPORT DATE	2. REPORT TYPE	3. DATES COVERED
01 JUN 2006	**N/A**	**-**

4. TITLE AND SUBTITLE	5a. CONTRACT NUMBER
Review of the Current Status of Four-Dimensional Ionospheric Imaging	5b. GRANT NUMBER
	5c. PROGRAM ELEMENT NUMBER
6. AUTHOR(S)	5d. PROJECT NUMBER
	5e. TASK NUMBER
	5f. WORK UNIT NUMBER
7. PERFORMING ORGANIZATION NAME(S) AND ADDRESS(ES) **Applied Research Laboratories The University of Texas at Austin USA**	8. PERFORMING ORGANIZATION REPORT NUMBER
9. SPONSORING/MONITORING AGENCY NAME(S) AND ADDRESS(ES)	10. SPONSOR/MONITOR'S ACRONYM(S)
	11. SPONSOR/MONITOR'S REPORT NUMBER(S)

12. DISTRIBUTION/AVAILABILITY STATEMENT
Approved for public release, distribution unlimited

13. SUPPLEMENTARY NOTES
See also ADM002065., The original document contains color images.

14. ABSTRACT

15. SUBJECT TERMS

16. SECURITY CLASSIFICATION OF:			17. LIMITATION OF ABSTRACT	18. NUMBER OF PAGES	19a. NAME OF RESPONSIBLE PERSON
a. REPORT	b. ABSTRACT	c. THIS PAGE			
unclassified	**unclassified**	**unclassified**	**UU**	**18**	

Standard Form 298 (Rev. 8-98)
Prescribed by ANSI Std Z39-18

ray tomography and produces images of the electron-density distribution. In the case of ionospheric tomography, the basic measurement is the total electron content (TEC). These measurements are taken along many intersecting raypaths between a satellite in low-Earth-orbit (LEO) and a chain of ground-based receivers. Total electron content, I_S, is defined as the line integral of the electron density along a radio-wave propagation path from a satellite, *S*, to a receiver, *R*. The TEC may be expressed as

$$I_s = \int_S^R N(r,\theta,\phi)\, ds \qquad (1)$$

in which N is the electron density, r the radial distance from the centre of the Earth, θ is the latitude, ϕ the longitude and s the distance along the satellite-to-receiver ray path.

Two different satellite systems have been used for ionospheric tomography - the USA Navy Navigational Satellite System (NNSS) and the Russian CICADA satellites. Satellites in the NNSS configuration are in near-circular polar orbits at around 1100 km altitude. They transmit phase coherent signals at approximately 150 and 400 MHz. The Russian CICADA satellites are in an orbit approximately aligned with the geomagnetic meridian and can be used for ionospheric tomography in a similar manner to the NNSS. The radio signals transmitted from the satellite at the two different frequencies are received by a chain of ground-based receivers (Figure 1). The refractive effect of the ionosphere on the two trans-ionospheric radio waves results in a phase difference between them. This phase difference can then be related to the integrated amount of ionisation, or electron concentration, present along the propagation path. Obviously the individual TEC measurements contain no information about the spatial variation of the electron concentration along the ray path. Hence the task of finding the spatial distribution of electron concentration requires a tomographic solution.

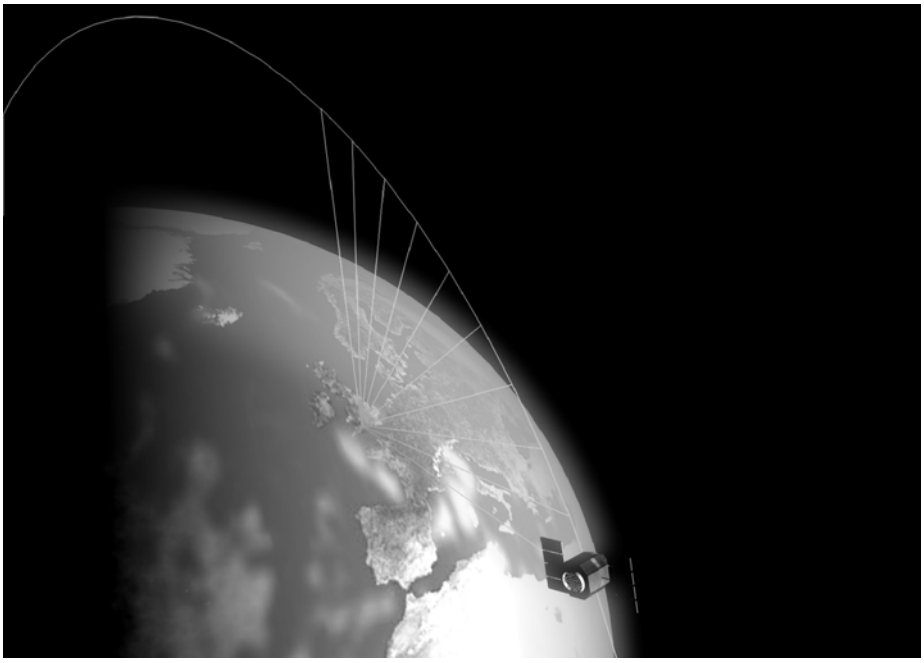

Figure 1. Diagram illustrating the geometry for ionospheric tomography. Only one receiver site is shown in the diagram for clarity.

The application of the tomographic technique to ionospheric imaging was first proposed in 1986 by Austen et al. and modelling studies presented by Austen et al. (1988) substantiated the idea. For this preliminary study they used an algorithm based on the finite-series expansion reconstruction technique. Such methods can be used with any ray-path geometry and are often the preferred option when the line integral data has been collected over a limited range of orientations (Censor, 1983). As an initial constraining condition for the algorithm, to compensate for the lack of vertical gradient information, the authors used a triangular vertical density profile with a peak density close to that in the simulation. These early simulations demonstrated the viability of ionospheric tomography.

Yeh and Raymund (1991) investigated some of the theoretical limitations of ionospheric tomography. The geometry in this LEO satellite-to-Earth configuration only allows observations over a limited number of viewing angles. In particular, the orientations of the satellite-to-receiver ray paths are biased in a vertical sense with no ray paths running horizontally through the ionosphere because of the curvature of the Earth. Consequently the vertical electron-concentration gradient is poorly defined by the TEC measurements alone. This geometrical constraint means that the reconstruction of the tomographic images is not straightforward and the reconstruction cannot be implemented directly using conventional inversion algorithms alone. This fact has contributed towards making ionospheric imaging a challenging research topic, bringing together mathematicians, physicists and engineers. There have been several algorithmic solutions, but the one described by Fremouw et al. (1992) is most widely used now. This algorithm, adapted from another geophysical application, uses a set of vertical orthonormal vectors, created from ionospheric models, to image the vertical profile and a power law spectrum to select the horizontal structures from a Fourier basis.

The first experimental result showing a tomographic image of the ionosphere was published by Andreeva et al. (1990). These authors, from the Moscow State University, used TEC data collected at three receivers located at Murmansk (68.6°N, 31.8°E), Kem (65.0°N, 34.6°E) and Moscow (55.7°N, 37.6°E). However, for these preliminary tomographic results no other local measurements of the ionospheric electron density were available for comparison with the reconstruction and it was not until 1992 (Pryse and Kersley) that a tomographic image with independent verification was published. This verification was provided by a scanning experiment of the European Incoherent Scatter (EISCAT) radar. Subsequent co-ordinated studies between tomographic imaging and the EISCAT radar have contributed hugely to the general acceptance of the tomographic technique.

Once tomographic imaging had been accepted as a viable technique it became credible that it could be used not only for scientific study and also for practical applications. Bust et al. (1994) investigated the application of ionospheric tomography to single site location range estimation; the determination of the location of an unknown transmitter. Heaton et al. (2001) and Rogers et al. (2001) have demonstrated the use of tomographic imaging in characterising HF radio communications paths.

Many ionospheric phenomena have been imaged using tomography. Images showing traveling ionospheric disturbances (TIDs) (Pryse et al. 1995; Cook and Close, 1995) have been presented. These waves-like structures are the manifestation of internal atmospheric gravity waves in the ionosphere. Mitchell et al. (1995) presented tomographic images of magnetic-field-aligned irregularities and E-region enhancements in the auroral region above northern Scandinavia. Kersley et al. 1997 demonstrated that the technique could be used to make images of large-scale ionisation depletions known as troughs, generally found on the night-side auroral mid-latitude boundary. An example of a tomographic image of the trough during very disturbed ionospheric storm conditions is shown in Figure 2. Results from the polar regions have indicated ionospheric signatures of processes occurring further out in space, such as magnetic reconnection events (Walker et al. 1998). A novel idea by Bernhardt et al. (1996) proposed the inclusion of measurements taken from natural

extreme ultraviolet emissions in the ionosphere into tomographic inversions. These satellite-based observations can provide vertical O^+ profiles, which are essentially the same as the electron-density profiles at F-layer heights.

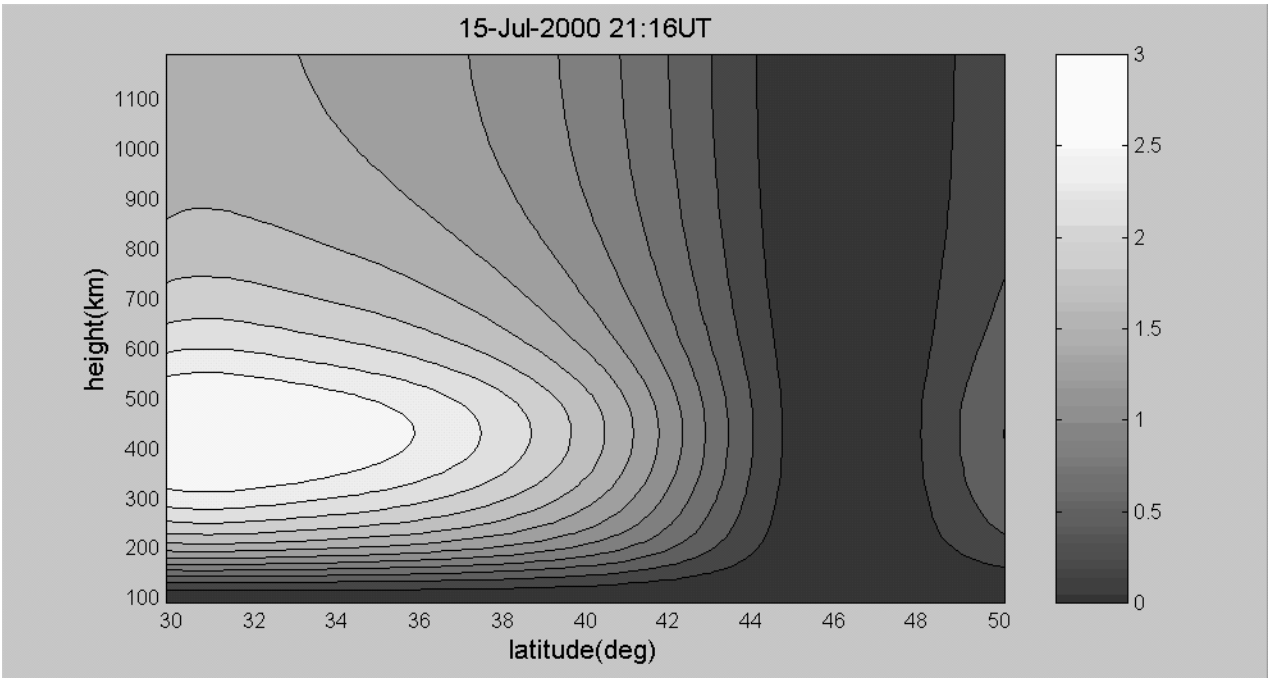

Figure 2. Tomographic image showing contours of electron concentration ($x10^{11}$ m^{-3}) outlining the main trough (after Spencer and Mitchell, 2001).

3.0 REVIEW OF CURRENT STATE OF IONOSPHERIC IMAGING

Information about ionospheric electron concentration can be derived from a range of different instruments. New opportunities are provided by the Global Positioning System (GPS) satellites. GPS consists of 24 satellites that transmit L-band radio signals at 1.575 and 1.228 GHz. Dual-frequency GPS signals can be recorded at ground-based receivers to obtain the signal's relative phase shift and delay. The dispersive nature of the ionospheric component allows the ionospheric delay to be determined separately from effects caused by propagation through the non-ionised part of the atmosphere. This provides information that can be related directly to TEC. GPS signals are providing an important and inexpensive new tool for ionospheric measurement. Future possibilities of a European-lead navigation satellite system can only increase the quantity of observations. The utilisation of such navigation system satellites for ionospheric research has the advantage of being very cost effective – no new satellite is required and the transmissions are at present free to everyone. Moreover, the receivers are commercially available at low cost. However, from any observation site the satellites appear at changing and oblique angles. Consequently the observations of total electron content are each along a different line-of-sight and thus are very complicated to interpret. This provides a natural requirement for the development of the types of tomographic techniques already described in this article. The radio-occultation technique uses receivers located on Low-Earth-Orbit (LEO) satellites to monitor the phase changes of GPS signals. These radio-occultation experiments have already been very successful for

neutral atmospheric studies. Satellite measurements are now increasingly used for ionospheric work. Hajj et al. (1994) suggested using the satellite-to-satellite transmission of GPS to LEO satellite measurements in a tomographic framework to provide the so-called 'missing horizontal rays' and improve the vertical resolution. In addition, LEOs provide measurements over the oceans and into remote polar caps, thus enabling the ionosphere to be studied on a truly global-scale. Past and current LEO missions include GPS/MET and more recently OERSTED, SAC-C and CHAMP. Further plans for more radio-occultation satellites by the European Space Agency, and the joint USA-TAIWAN project for a constellation of such satellites known as COSMIC, will enable atmospheric and ionospheric measurements to be made well beyond the next decade. GPS navigation receivers on board satellites allow measurement of the amount of TEC between the satellite and the GPS satellites (Heise et al., 2002, Jakowski et al., 2003, Stankov et al., 2003). Such over satellite electron content (OSEC) can be used to image the topside ionosphere and plasmasphere. Other ground and space based data sets include incoherent scatter radars (ISRs), ionosondes, and satellite in-situ measurements of electron density.

An exciting new prospect for ionospheric imaging is to combine observations from many different instruments to characterise the ionosphere globally. Conventional ionospheric tomography only creates a two-dimensional image but the extension of this into three and four dimensional inversions to derive real-time movies of electron concentration (latitude, longitude, altitude, time) has now been achieved with the MIDAS and IDA3D algorithms (Spencer and Mitchell, 2001; Bust et. al, 2004). The development of MIDAS and IDA3D are discussed in the following two sections. It should be noted here that there are other techniques that use GPS data to investigate the ionosphere that range from modified tomographic imaging (e.g. Garcia-Fernandez et al, 2004; 2005) to assimilation into physical models (e.g. Hajj et al., 2004**).** The discussion of these is beyond the scope of this paper.

3.1 MIDAS Development

The MIDAS algorithms are based upon the oceanographic imaging techniques of Munk and Wunsch (1979); first applied to imaging 2D slices of the ionosphere by Fremouw et al (1992). This was conventional tomographic imaging where the line integral data were approximated into a plane and inverted to reveal the electron density. MIDAS is a linear inversion algorithm that can ingest any line-integral data such as GPS-ground or GPS-LEO differential-phase data (Yin et al., 2005) or inverted ionograms.

The development of the MIDAS algorithms was driven by the success of two-dimensional ionospheric tomography for both scientific and applications work (e.g. Mitchell et al., 1995; Mitchell et al., 1998 and Rogers et al., 2001). Initially it was thought that GPS data could only be used for simple constant altitude shell mapping and early work concentrated in this area. Comparisons between shell mapping and full 3-D imaging can be found in Meggs et al., 2004. In fact, the step from 2-D shell mapping to full 3-D imaging is a matter of including mathematical concepts from tomography (Mitchell, 2002; Mitchell and Spencer, 2003). It was apparent that the differential phase-technique could only work with a time dependent algorithm, because the ionosphere changes while the satellite moves. Alternatively, pre-calibration of the differential code data could allow a time independent approach. Extensive simulation studies were used in the development of the techniques for the equatorial region and the mid-latitudes (Meggs et al., 2004). At higher latitudes images of the main trough have been verified by incoherent scatter radar (Meggs et al., 2005). The imaging has recently been applied to the sparse-data region of South Africa (Cilliers et al., 2004)

The first stage of the MIDAS algorithm (Mitchell and Spencer, 2003) inversion is to set up a three-dimensional grid of voxels, each bounded in latitude, longitude and altitude, and to compute the length of each element of a satellite-to-receiver signal propagation path though each intersected voxel. The unknown

electron concentration, $\mathbf{x_a}$, is defined to be constant within each voxel and contained in the column vector. The problem may now be expressed as,

$$\mathbf{y} = \tilde{\mathbf{H}}\mathbf{x_a} \qquad (2)$$

where the matrix **H** transforms the electron density to the form and location of the observations and **y** are the observed TECs. It should be noted that the inversion uses relative differential phase observations. Thus appropriate lines of the matrix are differenced such that measurements along continuous satellite-receiver arcs are taken relative to a certain reference measurement within that arc.

The inversion cannot be performed directly so a mapping matrix, **X**, is used to transform the problem. This results in a situation where the unknowns are coefficients of orthonormal basis functions, the combination of which will give the final image of electron concentration. The basis functions (**X**) can be generated using a spherical harmonic expansion to represent the horizontal variation and empirical ortho-normal functions (EOFs) for the radial variation in electron concentration. The spherical harmonics provide a flexible basis to determine the horizontal distribution of ionization, which should be well defined by the measurements. The EOFs form a constraint to the vertical profile, only allowing a certain range of possible solutions.This is now expressed mathematically as

$$\mathbf{y} = \tilde{\mathbf{H}}\tilde{\mathbf{X}}\tilde{\mathbf{W}} \qquad (3)$$

where the matrix **X** contains the basis functions. **HX** now represents the set of TEC data that are formed by integration through the set of models. Applying singular value decomposition the inversion can be performed such that

$$\tilde{\mathbf{W}} = (\tilde{\mathbf{H}}\tilde{\mathbf{X}})^{-1}\,\mathbf{y} \qquad \mathbf{(4)}$$

and the solution to the inverse problem is then given by

$$\mathbf{x_a} = \tilde{\mathbf{W}}\tilde{\mathbf{X}} \qquad (5)$$

The algorithm can be extended into a time-dependent inversion by incorporating a priori information about the evolution of the electron concentration during a specified period of time. Assuming that the change in electron concentration within a voxel with time is linear, then it is possible to write the same system of equations to solve for the change in the relative contributions of each basis function.

3.2 IDA3D Development

ARL:UT began developing two-dimensional tomographic images of the ionosphere using LEO satellites in 1991. From 1993 – 2002 several experimental campaigns were conducted using a single array of receivers, and multiple arrays (Bust et al., 1994; Kronschnabl et al., 1995). Starting in 1996 (Coker, 1997a and b) regional three-dimensional images of the ionosphere were obtained by combining two-dimensional images obtained from computerized ionospheric tomography (CIT) with GPS vertical total electron content (VTEC).

While such an approach was useful as an initial method of combining different data sources, and led to a better understanding of how different data sources impact the 3D inversion, the technique was somewhat limiting and *ad-hoc*. Thus an algorithm that could accept any kind of electron content measurement was developed. This would include line-of-sight GPS TEC, CIT beacon TEC and low earth orbiting (LEO) GPS TEC. Like the previous algorithm, the new algorithm updated its specification of the regional electron density at regular time intervals. Starting in 1998 (Bust et al., 2000; 2001a and b) the development of the current algorithm IDA3D began. IDA3D uses a maximum likelihood minimization of a cost function, where the *a-priori* information consists of data and model error covariances, and the background model state. IDA3D can be run either globally and regionally on a large number of different data sets. It is highly user-configurable being designed more for the investigation of science than operational requirements.

The Ionospheric Data Assimilation Three Dimensional (IDA3D) (Bust et. al., 2004) is an objective analysis algorithm, based upon three dimensional variation (3DVAR) data assimilation. This mathematical technique (Daley and Barker, 2000, Daley, 1991) is similar to a least-squares fit between the full set of observations and a background specification. As with all analysis algorithms, the observations are interpolated onto a predetermined grid, which allows the measurements to be shown collectively and for larger scale (larger than a single observation) phenomena to be observed. 3DVAR not only uses the specification and observation errors, but also includes the correlation between grid points. In a perfect world, the observations would completely span the system, and 3DVAR (and hence IDA3D) would only be an interpolation algorithm. However, such data sets do not exist and a background specification is needed to complete the system.

IDA3D works by solving the standard 3DVAR equations for ionospheric electron density

$$\mathbf{x_a} = \mathbf{x_f} + \tilde{\mathbf{P}}_\mathbf{f}\tilde{\mathbf{H}}^\mathbf{T}\left[\tilde{\mathbf{R}} + \tilde{\mathbf{H}}\tilde{\mathbf{P}}_\mathbf{f}\tilde{\mathbf{H}}^\mathbf{T}\right]^{-1}\left(\mathbf{y} - \tilde{\mathbf{H}}\mathbf{x_f}\right) \qquad (6)$$

$$\tilde{\mathbf{P}}_\mathbf{a} = \tilde{\mathbf{P}}_\mathbf{f} - \tilde{\mathbf{P}}_\mathbf{f}\tilde{\mathbf{H}}^\mathbf{T}\left[\tilde{\mathbf{R}} + \tilde{\mathbf{H}}\tilde{\mathbf{P}}_\mathbf{f}\tilde{\mathbf{H}}^\mathbf{T}\right]^{-1}\tilde{\mathbf{H}}\tilde{\mathbf{P}}_\mathbf{f} \qquad (7).$$

Where $\mathbf{x_a}$ is the analysis electron density at a given time, $\mathbf{x_f}$ is the forecast electron density for that time, $\mathbf{y}$ is the set of electron density and electron content observations, $\mathbf{P_f}$ is the error covariance matrix for the forecast model, $\mathbf{R}$ is the error covariance matrix for the observations, and the matrix $\mathbf{H}$ transforms the predicted electron density to the form and location of the observations. The forecast electron density and error covariance matrix are specified as

$$\mathbf{x_f}(t_{n+1}) = e^{-\frac{\Delta t}{\tau}}\left(\mathbf{x_a}(t_n) - \mathbf{x_b}(t_n)\right) + \mathbf{x_b}(t_{n+1}) \qquad (8)$$

$$\tilde{\mathbf{P}}_\mathbf{f}(t_{n+1}) = (1 - e^{-\frac{2\Delta t}{\tau}})\tilde{\mathbf{P}}_\mathbf{b}(t_n) + e^{-\frac{2\Delta t}{\tau}}\tilde{\mathbf{P}}_\mathbf{a}(t_n) \qquad (9).$$

Where $\mathbf{x_b}$ is the specification from a background electron density model, τ is the estimated correlation time, t_{n+1} is the present time step, t_n is the previous time step, and $\mathbf{P_b}$ is the error covariance matrix for the background electron density model. The observation vector $\mathbf{y}$ contains all available data sets that can be incorporated into IDA3D. The transformation matrix $\mathbf{H}$, contains the information necessary for predicting the value of the observation from the forecast density vector. The error covariance matrices represent the error

between the analysis, observation, or background and the true value of the electron density and the correlation between any two given observations or grid points. It can be separated into an error variance matrix, which is a diagonal matrix, and a correlation matrix between different observations or grid points.

To solve equations 6 and 7, IDA3D needs certain inputs. These include background climatology with a model grid, electron density specification, correlations, and a set of observations (direct measurements, or radiances from remote sensing) that is easily related to the electron density. The model grid is an input that is chosen for its compatibility with the specific scientific investigation that is planned. It should be noted that IDA3D is not rigidly linked to any background model. Typically the International Reference Ionosphere (Bilitza, 2001) is used, or a first principle model such as the Thermosphere-Ionosphere-Mesosphere-Electrodynamic General Circulation Model (TIME-GCM) (Roble and Ridley, 1994). The impact of the background model is significantly reduced by application of the Gauss-Markov Kalman filter technique (Gelb, 1974) (Equations 8 and 9). The background model error correlations are treated as inputs that are independent of the background model. At present, the correlations are treated as correlation lengths in latitude, longitude and altitude. The background model correlations decrease exponentially as the ratio of the distance between the model points and the correlation length. The horizontal and vertical distances are treated separately. In addition, a correlation time is given as input. These correlations allow the data to impact a larger region of the specification than just of the grid points affected by the observations and allow past observations to impact the present specification.

3.3 Science with ionospheric imaging

Here we briefly describe several scientific studies that 4D ionospheric imaging has significantly contributed to.

A study of the evolution and fate of polar cap patches was undertaken by Bust and Crowley (Bust and Crowley, 2006) for the period on December 12, 2001 1800-2300 UT. During this period the EISCAT Svalbard Radar (ESR) observed a sequence of polar patches. Low Densities ($Ne < 4.0*10^{11}$ el/m^3) at 350 km were observed for several hours, followed by a sequence of electron density enhancements between 2000—2130 UT, with another broader structure from 2130--2215 UT. The question addressed by this study was what was the source of the observed patches? To investigate this question, IDA3D imaging was performed every 5 minutes over a 24 hour period on this day with TIME-GCM as the background model. Figure 3 below shows an IDA3D image taken at 350 kilometer altitude at 21 UT, during the time of patch observations. Note the narrow filament of high plasma density extending into the ESR field of view. Detailed analysis of the transport using these combined techniques demonstrated that the patch structures observed by the ESR originated along the morning (and in one case dusk) cells of the convection pattern. These were convected into sunlight where the plasma density was enhanced above $1.0*10^{12}$ el/m^3, and was subsequently transported across the polar cap, distorted into long narrow filaments of plasma, and observed by the ESR.

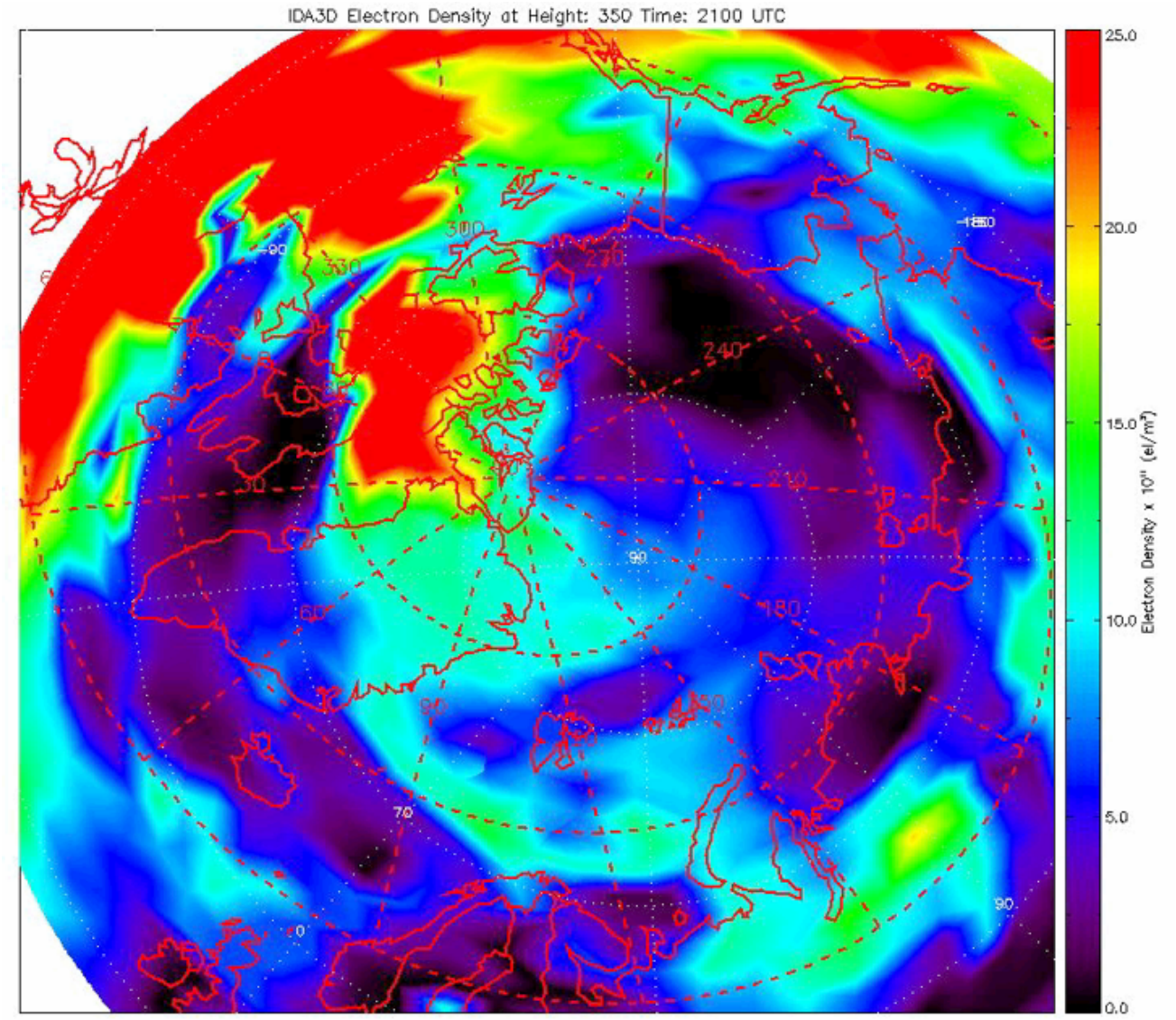

Figure 3. Section of an IDA3D image taken at 350 km altitude at 2100 UT.

One of the advantages of 4D imaging is the capability to investigate the plasma distribution on spatial and temporal scales ranging from 10s of kilometers to the globe spatially, and from a few minutes to days temporally. In addition, such investigations can be studied from a number of different look directions, allowing better elucidation of the underlying plasma structure. To illustrate this we present IDA3D results over the USA taken from Oct 30, 2003 at 0600 UT in figures 4 and 5 below. Figure 4 shows re-integrated vertical TEC obtained from IDA3D. This time period is after the large storm enhanced density (SED) of the previous day has swept across the USA. 0600 UT is ~ local midnight in this longitude sector. Yet, as the ionospheric plasma density decayed with the onset of post-sunset, a elongated narrow plume of higher density plasma persisted across the southwest USA. Other data sets taken from a tomography receiver located at Austin Texas, DMSP over flights, and raw slant GPS TEC data from stations in the region all confirm that this

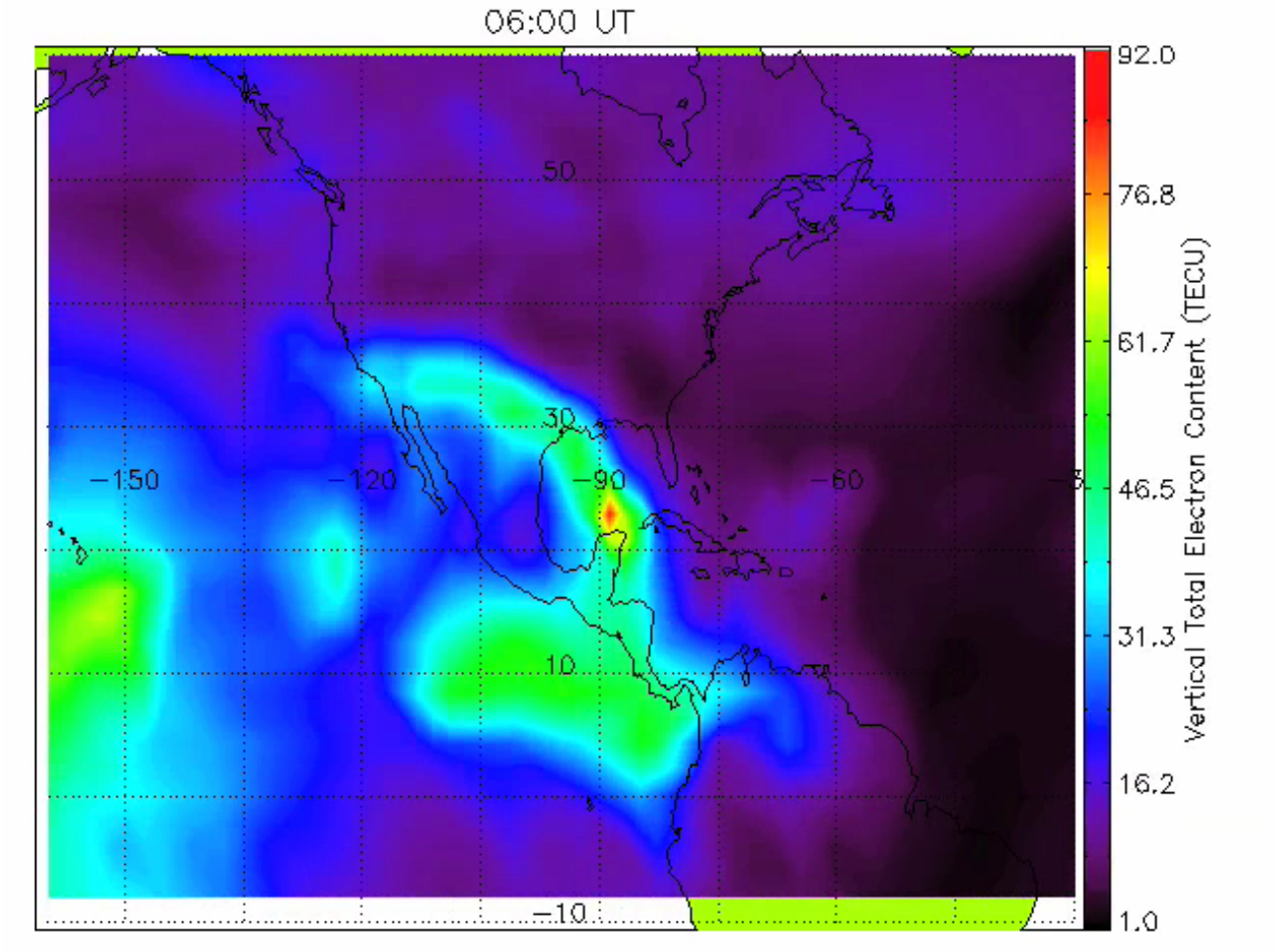

Figure 4. IDA3D vertical TEC over the USA. The image is taken at 0600 UT on October 30, 2003. The scale is in log10 electron density.

enhanced plume of plasma density is a real effect. To better understand the structure of this enhanced density a 2D slice in latitude and altitude was taken along the 260 degree longitudes. The results are presented in figure 5. It is interesting that the enhanced plasma has been lifted up to 500-800 km altitude between 28-30 degrees latitude. In addition, just southward of the enhancement, at 25 degrees latitude, there seems to be a significant depletion from 700 km altitude and below. Further study of this event, combined with theoretical modelling will hopefully elucidate the underlying physics producing the observed plasma structure.

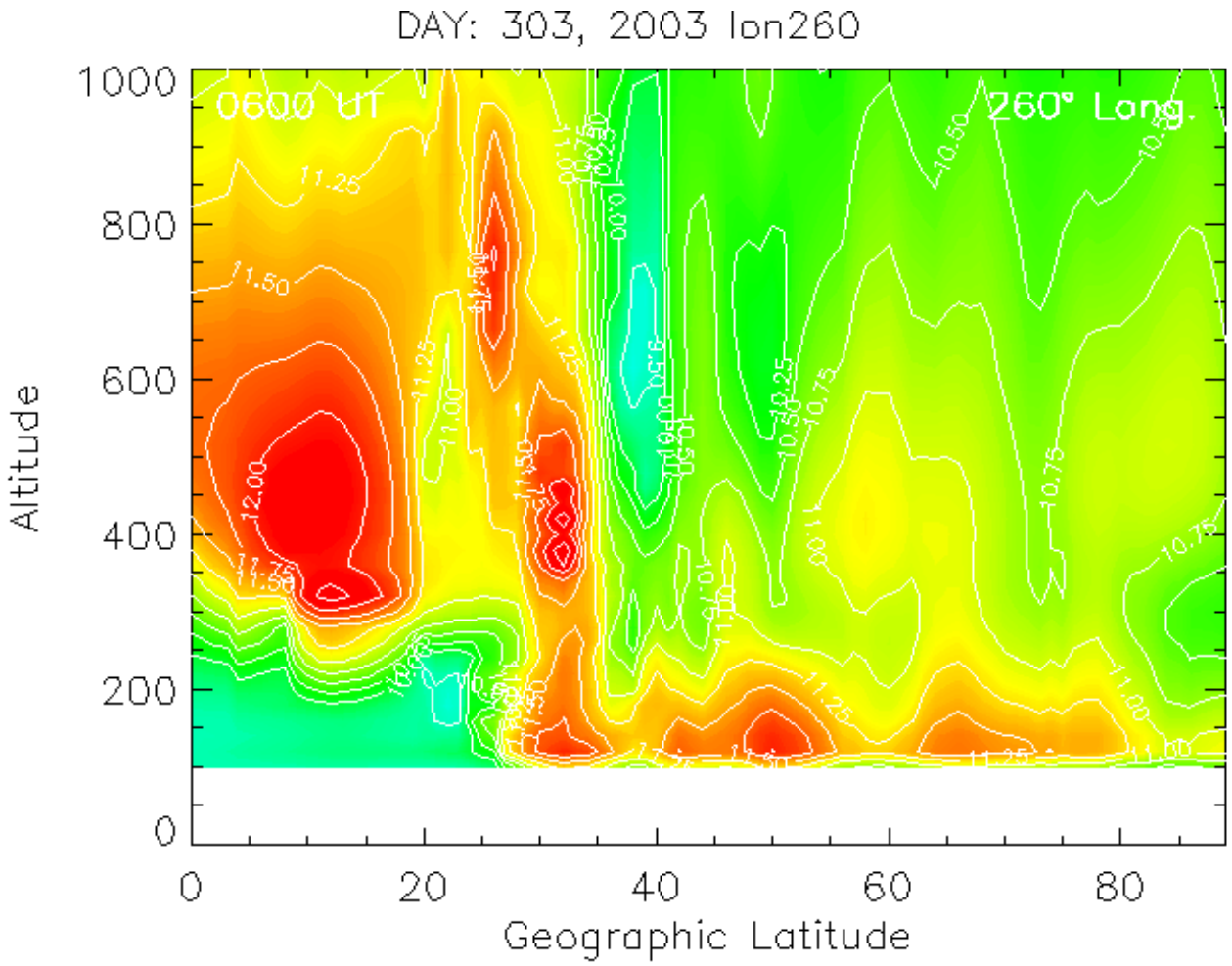

Figure 5. A altitude – latitude slice at 260 degrees longitude through the same IDA3D result as presented in figure 4 above.

4.0 LIMITATIONS AND FUTURE DIRECTIONS

4.1 Current Limitations of 3D dynamical tomographic imaging of electron density

Ionospheric tomographic imaging is a mixed-determined, limited-angle tomographic inverse problem. By mixed-determined we mean there are regions where the data over-determines parts of the solution, and regions where the solution is under-determined. By limited angles, we mean that we do not have complete coverage of data, from all possible directions. For ionospheric imaging, we generally do not have good measurements in directions perpendicular to altitude, so the altitude resolution is not as good as the horizontal resolution. These two issues drive practical limitations in the ionospheric imaging solutions. First, lack of data is certain regions, implies that the tomographic solution is not uniquely determined by the data alone. This in turn implies that some kind of a-priori information must be added to uniquely determine the result. If the a-priori information is ad-hoc in some way, or not based on strong physical arguments, or if the imaging results depend strongly on the a-priori information, then a limitation to the accuracy of the results is obtained.

Second, limited angles in the altitude direction imply limitations on the vertical (radial) resolution in the imaging.

Both of these limitations are currently being addressed by the availability of new data sources. Global ground-based GPS data networks have greatly improved our overall data coverage. Satellite-based observations such as the recently launched COSMIC satellites provide additional data, especially over oceans that improve global data-coverage and reduce the necessity for a-priori information. Satellite in-situ measurements of electron density, and occultation measurements provide observations that have good altitude information in them, and help reduce the limited angle limitations. Thus, the two major limitations in accuracy and resolution in 3D dynamical tomographic imaging are being addressed by the continuing deployment of additional data. We expect this increase in available data will continue into the next several years, further improving the accuracy and resolution of the imaging results.

4.2 Future Directions

Future opportunities are promising for this imaging work. The new European satellite navigation system, Galileo, will double the quantity of TEC data, increasing the coverage for such imaging within the next few years. There are also more occultation satellites planned, most notably COSMIC that will become operational later this year. These will increase the coverage of the topside ionosphere data that is so important for vertical resolution in the images.

In terms of the techniques themselves exciting opportunities exist for gaining a much deeper understanding of the physical drivers behind the processes that can be observed. A new approach is currently being investigated by the authors for studying the ionosphere directly using time dependent 3D images to directly estimate the important physical drivers producing the images.

5.0 DISCUSSION

The development and implementation of two different imaging algorithms has been described. Each algorithm builds upon well established 2D tomographic imaging techniques. They have both been verified in special campaign case studies with collocated incoherent scatter radars at both high and mid-latitudes.

The main focus of the paper has been on the actual use of 4D imaging as a tool for scientific investigations. It should be emphasized that the GPS data have been available continuously for about a decade now and that here, only a few highlights have been chosen to demonstrate the ways that it can be used. At high latitudes, where the data are sparse the combination of images with models can be used to investigate the transport of patches across the polar cap. At mid-latitudes, where the data are more dense over the continental regions of North America and Europe, data-rich images of the ionosphere are not so reliant on models and can reveal remarkable changes in the usual plasma dynamics.

For the case study storm of October 2003 the overall analysis demonstrates a coordinated set of observations obtained from MIDAS and IDA3D that extend from the equatorial region in the American sector, through mid-latitudes all the way across the polar-cap to the midnight sector over EISCAT. By using both 4D imaging methods together, they reinforce the results providing confidence in the results of each technique. It is only through such 4D imaging methods that such a large scale global analysis of the ionospheric response to a major geomagnetic storm can be obtained.

Future opportunities are promising for this imaging work. The new European satellite navigation system, Galileo, will double the quantity of TEC data, increasing the coverage for such imaging within the next few years. There are also more occultation satellites planned, most notably COSMIC, that will become operational later this year. These will increase the coverage of the topside ionosphere data that is so important for vertical resolution in the images.

In terms of the techniques themselves exciting opportunities exist for gaining a much deeper understanding of the physical drivers behind the processes that can be observed. A new approach is currently being investigated by the authors for studying the ionosphere directly using tomographic images. Initially a tomographic movie is made and then a physical model is run with many different driving parameters to find those which best allow the model to replicate the movie. Given that the images are 3D, continuous in time and cover wide spatial regions, this approach constrains the model much more than conventional data assimilation of TEC.

Acknowledgements: The instrumentation for the Greenland tomography array was built and deployed through the National Science Foundation under Grant ATM-9813864. Development of IDA3D was supported by the Office of Naval Research under grant N00014-97-1-0236. IDA3D investigations of the equatorial ionosphere and polar-cap were supported through the National Science Foundation under Grants ATM-0513826 and ATM-0228467 respectively. The authors from ARL:UT are grateful to Werner Singer and Jens Mielich for providing the Juliusruh/Ruegen digisonde data, Terrence Bullett and the Air Force Research Laboratories for providing data from the Digital Ionospheric Sounding System, Bodo Reinsch and Ivan Galkin for providing data from the data from the Digital Ionosonde Database, Cesar Valladares for GPS data from his chain of South American stations, Dave Cooke for providing the CHAMP in situ data, and S. Y. Su for providing the ROCSAT electron densities. Additionally, the authors wish to thank the International GPS Service, the Scripps Orbit and Permanent Array Center, and the Continuously Operating Reference Stations network for providing online GPS data; Eric Kihn and the Space Physics Interactive Data Resource at the National Geophysical Data Center for provide web accessible peak height measurements from digisonde and geomagnetic indices; the Coordinated Data Analysis Web at Goddard Space Flight Center for provide the POLAR data; the University of Texas at Dallas for providing the online DMSP database; NASA's Global Environmental and Earth Science Information System for providing the satellite-based GPS measurements, and the Open Madrigal Initiative for provide incoherent scatter radar data. We are grateful to GFS for the use of CHAMP data and JPL for releasing SAC-C data. Topex and GRACE data were obtained from the Physical Oceanography Distributed Active Archive Center (PO.DAAC) at JPL.

The AMIE technique depends on data provided by many individual experimenters and data centers. We are grateful for SuperDARN radar data from Mike Ruohoniemi (Goose Bay and Kapuskasing), George Sofko (Saskatoon), Jean-Paul Villain (Stokkseyri) and Mark Lester (CUTLASS and Hankasalmi). The Goose Bay and Kapuskasing SuperDARN radars are operated by the Applied Physics Laboratory of The Johns Hopkins University with support from the National Science Foundation. The Saskatoon HF radar is operated by the University of Saskatchewan with support from the Natural Sciences and Engineering Research Council of Canada. The CUTLASS (Co-operative UK Twin Located Auroral Sounding System) and Hankasalmi radars form part of the SuperDARN (Dual Auroral Radar Network) network, and are operated by the Radio and Space Plasma Physics Group at the University of Leicester with support from the Particle Physics and Astronomy Council, and additional support from the Finnish Meteorological Institute and the Swedish Meteorological Institute. The Stokkseyri HF radar is operated by CNRS/LPCE (Centre National de la Recherche Scientifique/ Laboratoire de Physique Chimie de l'Environnement) and CNRS/CETP (Centre d'etudes des Environnements Terrestre et Planetaires) with support from the Institut National des Sciences de l'Univers. The Defense Meteorological Satellite Program ion velocity data were provided by Fred Rich of the Air Force Research Laboratory and Rod Heelis/Marc Hairston of the University of Texas at Dallas. TIME-GCM was developed at the National Center for Atmospheric Research.

CNM is grateful to the UK research councils EPSRC and PPARC and to BA SYSTEMS for supporting this work. The use of data provided by the International GPS Service (IGS) and by Brasileiro de Geografia e

Estatistica (IBGE) is acknowledged. The Sondrestrom incoherent scatter radar is supported by the National Science Foundation. We are indebted to the Director and staff of EISCAT for operating the facility and supplying the data. EISCAT is an international association supported by Finland (SA), France (CNRS), Germany (MPG), Japan (NIPR), Norway (NFR), Sweden (VR) and the United Kingdom (PPARC).

6.0 REFERENCES

[1] Andreeva, E.S., A.V. Galinov, V.E. Kunitsyn, Yu.A. Mel'nichenko, E.D. Tereshchenko, M.A. Filimonov, and S.M. Chernykov, 1990, Radio tomographic reconstruction of ionisation dip in the plasma near the Earth, *J. Exp. Theor. Phys. Lett*., **52**, 145.

[2] Austen, J.R., S.J. Franke, C.H. Liu, and K.C. Yeh, 1986, Application of computerized tomography Techniques to ionospheric research, *Proc. International Beacon Satellite Symposium*, **25**, Oulu, Finland.

[3] Austen, J.R., S.J. Franke, and C.H. Liu, 1988, Ionospheric imaging using computerised tomography, *Radio Science*, **23**, 299.

[4] Bernhardt, P.A., K.F. Dymond and J.M. Picone, 1996, Improved radio tomography of the ionosphere using EUV/optical instruments from satellites, *Proc. Ionospheric Effects Symposium, Alexandria, USA.*

[5] Bilitza D, International Reference Ionosphere 2000, Radio Science, 36 (2): 261-275 MAR-APR 2001

[6] Bracewell, R.N., 1956, Strip integration in radio astronomy *Aust. J. Physics***, 9**, 198.

[7] Bust, G. S., J. A. Cook, G. R. Kronschnabl, C. J. Vasicek, and S. B. Ward, Application of Ionospheric Tomography to Single-Site Location Range Estimation, J. Img. Sys. Tech., Vol 5, 1994

[8] Bust, G.S., D. Coco and J. Makela, "Combined Ionospheric Campaign 1: Ionospheric Tomography and GPS total electron count (TEC) Depletions", 27(18) Geophys. Res. Lett., 2000

[9] Bust, G.S., D.S. Coco and T.L. Gaussiran II, Computerized Ionospheric Tomography Analysis of the Combined Ionospheric Campaign, 36(6), Radio Science, 2001a

[10] Bust, G.S., C. Coker, D. Coco, T.L. Gaussiran II and T. Lauderdale, "IRI Data Ingestion and Ionospheric Tomography", 27(1) Adv. Space Res., 2001b

[11] Bust G. S., T. W. Garner, T. L. Gaussiran II, Ionospheric data assimilation three-dimensional (IDA3D): A global, multisensor, electron density specification algorithm, Journal of geophysical research-space physics 109 (a11): art. No. A11312 Nov 27 2004

[12] Bust, G.S. and G. Crowley, Tracking of Polar Cap Ionospheric Patches, submitted, J. Geophys. Res., 2006

[13] Censor, Y., Finite series expansion methods, 1983, *Proc. I.E.E.E*., **71**, 409.

[14] Cilliers P. J., Opperman B. D. L., Mitchell C. N., Spencer P. S. J., Electron density profiles determined from tomographic reconstruction of total electron content obtained from GPS dual frequency data: First results from the South African network of dual frequency GPS receiver stations, IRI: Quantifying Ionospheric Variability Advances In Space Research 34 (9)2049-2055 2004

[15] Coker C., Investigation of 22-23 Oct 96 Ionospheric Storm Using 3D Tomography, Austin CIT Conference, ARL:UT, Austin, TX, February 4-6, 1997a.

[16] Coker C., Specifying the Ionosphere in 4D Using CIT and GPS Sensors, Space Weather: Research to Operations Workshop, NOAA Space Environment Center, Boulder, CO, January 16-17, 1997b.

[17] Cook, J.A., and S. Close, An investigation of TID evolution observed in MACE '93 data, 1995, *Ann. Geophysicae*, **13,** 1320.

[18] Daley R., Atmospheric Data Analysis, Cambridge University Press, Cambridge, 1991

[19] Daley R., and E. Barker, The NAVDIS source book 2000: NRL Atmospheric Variational Data Assimilation System, NRL Publication, NRL/PU/7530-00-418, Naval Research Laboratory, Monterey, Ca., 2000

[20] Foster, J.C., and W. Rideout, Midlatitude tec enhancements during the October 2003 superstorm, Geophys. Res. Lett., 32, doi:10.1029/2004GL021,719,2005

[21] Fremouw, E.J., J.A. Secan and B.M. Howe, 1992, Application of stochastic inverse theory to ionospheric tomography, *Radio Science*., **17**, 721.

[22] Garcia-Fernandez M., Hernandez-Pajares M., Juan J.M., Sanz J., Improvement of ionospheric electron density estimation with GPSMET occultations using Abel inversion and VTEC information, Journal Of Geophysical Research-Space Physics 109 (A4): Art. No. A04302 APR 3 2004

[23] Gelb, A., Applied Optimal Estimation, MIT Press, Cambridge, Mass, 1974

[24] Garcia-Fernandez M., Saito A., Juan J.M., Tsuda T., Three-dimensional estimation of electron density over Japan using the GEONET GPS network combined with SAC-C data and ionosonde measurements, Journal Of Geophysical Research-Space Physics 110 (A11): Art. No. A11304 NOV 11 2005

[25] Hajj G.A., Wilson B.D., Wang C., Pi X., Rosen I.G., Data assimilation of ground GPS total electron content into a physics-based ionospheric model by use of the Kalman filter, Radio Science 39 (1), art. no. rs1s05 feb 24 2004

[26] Heaton JAT, Cannon PS, Rogers NC, Mitchell CN, Kersley L, 2001, Validation of electron density profiles derived from oblique ionograms over the United Kingdom, *Radio Science* ,**36** (5), 1149

[27] Heise, S., N. Jakowski, A. Wehrenpfennig, C. Reigber, and h. Luhr, Sounding of the topside ionosphere/plasmasphere based on GPS measurements from CHAMP: Initial results, Geophys. Res. Lett., 29, doi:10.1029/2002GL014738, 2002

[28] Hounsfield, G.N., 1972, A method of and apparatus for examination of a body by radiation such as X-ray or gamma radiation, Patent Specification 1283915, The Patent Office.

[29] Jakowski, N., S. Heise, K. Tsybulya, and A. Wehrenpfennig, Sounding the ionosphere by GPS measurements on CHAMP, Geophysical Research Abstracts, 5, 2003

[30] Kersley L, Pryse SE, Walker IK, Heaton JAT, Mitchell CN, Williams MJ, Willson CA, 1997, Imaging of electron density troughs by tomographic techniques, *Radio Science*, **32** (4): 1607.

[31] Kirchengast, G., The Graz ionospheric flux tube model, STEP handbook on ionospheric models, Utah State University, 1996

[32] Kronschnabl, G., G.S. Bust, J.A. Cook and C.J. Vasicek, Mid-America computerized ionospheric tomography experiment (MACE '93), Radio Sci., 30(1),105-108 (1995)

[33] Materassi M. and Mitchell C.N., Imaging of the equatorial ionosphere, Annals Of Geophysics 48 (3): 477-482 JUN 2005

[34] Meggs R. W., Mitchell C.N., Spencer P. S. J., A comparison of techniques for mapping total electron content over Europe using GPS signals Radio Science 39 (1): Art. No. RS1S10 FEB 25 2004

[35] Meggs R.W., Mitchell C.N., Howells V.SC., Simultaneous observations of the main trough using GPS imaging and the EISCAT radar Annales Geophysicae 23 (3): 753-757 2005

[36] Mitchell, C.N., D.G. Jones, L. Kersley, S.E. Pryse and I.K. Walker, Imaging of field- aligned structures in the auroral ionosphere, Ann. Geophysicae, 13, 1311-1319, 1995.

[37] Mitchell C.N., Walker I.K., Pryse S.E., Kersley L., McCrea I.W., Jones T.B., First complementary observations by ionospheric tomography, the EISCAT Svalbard radar and the CUTLASS HF radar, Annales Geophysicae-Atmospheres Hydrospheres And Space Sciences 16 (11): 1519-1522 NOV 1998.

[38] Mitchell C.N. Imaging of near-Earth space plasma Philosophical Transactions Of The Royal Society Of London Series A-Mathematical Physical And Engineering Sciences 360 (1801): 2805-2818 DEC 15 2002

[39] Mitchell C.N., Spencer P.S.J. A three-dimensional time-dependent algorithm for ionospheric imaging using GPS ANNALS OF GEOPHYSICS 46 (4): 687-696 AUG 2003

[40] Mitchell C.N., Alfonsi L., De Franceschi G., Lester M., Romano V., Wernik A.W., GPS TEC and scintillation measurements from the polar ionosphere during the October 2003 storm, Geophysical Research Letters 32 (12): Art. No. L12S03 MAY 3 2005

[41] Munk, W., and C. Wunsch, Ocean acoustic tomography: A scheme for large scale monitoring, Deep Sea Res., 26A, 123, 1979.

[42] Pryse, S.E., and L. Kersley, A preliminary experimental test of ionospheric tomography, 1992, *J. Atmos. Terr. Phys*., **54,** 1007.

[43] Pryse, S.E, C.N. Mitchell, J.A.T. Heaton and L. Kersley, 1995, Travelling ionospheric disturbances imaged by tomographic techniques, *Ann. Geophysicae*, **13**, 1325.

[44] Radon, J., 1917, Uber die Bestimmung von Funktionen durch ihre Integralwerte längs gewisser mannigfaltigkeiten, Saechsische Berichte Akademie der Wissensxhaften, 69, 262.

[45] Rishbeth H., Ganguly S., and J.C.G. Walker, Field-aligned and field-perpendicular velocities in the ionospheric F2-layer, J. atmos. terr. Phys., 40, 1978

[46] Roble, R.G., and E.C. Ridley, A thermosphere-ionosphere-mesosphere-electrodynamics general circulation model (TIME-GCM): Equinox solar cycle minimum simulations (30-500 km), Geophys. Res. Lett., 21, 417-420, 1994

[47] Rogers N.C., Mitchell C.N., Heaton J.A.T., Cannon P.S., Kersley L., Application of radio tomographic imaging to HF oblique incidence ray tracing, RADIO SCI 36 (6): 1591-1598 NOV-DEC 2001

[48] Spencer PSJ and C N Mitchell, 2001, Multi-instument Data Analysis System, Proc. Beacon Satellite Symposium, Boston.

[49] Stankov, S.M., N. Jakowski, S. Heise, P. Muhtarov, I. Kutiev, and R. Warnant, A new method for reconstruction of the vertical electron density distribution in the upper ionosphere and plasmasphere, J. Geophys. Res., 108, doi:10.1029/2002JA009570, 2003

[50] Walker IK, Moen J, Mitchell CN, Kersley L, Sandholt PE, 1998, Ionospheric effects of magnetopause reconnection observed using ionospheric tomography, *Geophysical Research Letters*, **25** (3): 293.

[51] Yeh, K.C., and T.D. Raymund, 1991, Limitations of ionospheric imaging by tomography, *Radio Science*, **26**, 1361

[52] Yin P., Mitchell C.N., Spencer P.S.J., Foster J.C. Ionospheric electron concentration imaging using GPS over the USA during the storm of July 2000, Geophysical Research Letters 31 (12): Art. No. L12806 JUN 22 2004

[53] Yin P., Mitchell C.N. Use of radio-occultation data for ionospheric imaging during the April 2002 disturbances Source: GPS SOLUTIONS 9 (2): 156-163 JUL 2005